DETECTION OF NEOTECTONIC FEATURES USING HYPERSPECTRAL AND SAR DATA, AMAZIJAHU FAULT - DEAD SEA RIFT, ISRAEL

[*,**]**Shimoni Michal, *Van der Meer Freek**
[*]ITC - International Institution for Aerospace Survey and Earth Sciences
Geological survey division.
[**]SIC - Signal and Image Centre, Brussels
mshimoni@elec.rma.ac.be , vdmeer@itc.nl

[***]**Ben-Dor Eyal**
[***]Tel-Aviv University
Department of Geography and Human Environment
Bendor@post.tau.ac.il

[****]**Shulman Haim**
[****]Tel-Aviv University
Department of Geophysics and Planetary Sciences

Key Words: Hyperspectroscopy, SAR interferometry, Tectonism, Seismic profiles, Sediment displacement, ERS-1/2, DAIS-7915.

Abstract

The ERS-1/2 tandem mission opened a new dimension in the geology and the tectonic researches. Displacements of active tectonic structure can be detected by using the phase of the radar signal. However, the global understanding of neotectonic process as well as interpretation of the interferometry data require geophysical investigation and complete description of the geological setting. Regional geological mapping and mineral exploration are within the main targets of the hyperspectral technology. In areas were faults are covered by loose sediments, the surface mineralogy deposition is essential. Amazijahu fault is part of the Dead Sea rift, an active fracture zone with continuous seismic activity. The displacement along the fault has never been mapped and the geological setting has never been studied. By using new analysis technique and geophysical inversion models, the research extracted quantitative information about surface mineralogy from the DAIS-7915 data. By using SAR Interferometry we will measure the relative movement and its direction. Seismic analysis was used to decode the relationship between the deep seismic activity and the surface cover. The combination of data will be used to produce a model detecting minor neotectonic faults in the Dead Sea Rift, southern basin, Israel. This article presents some preliminary results of combining seismic and advanced remote sensing data. Agreement between seismic activity and lithological distribution was found in the Dead Sea rift.

1 Introduction

The recognition of tectonic signatures within the sedimentary rock record gives important insights into the evolution of the surface morphology at a various scales. Evidence of tectonism is held within the geometry of the fill and within the sedimentary pile at the megasequence scale. At a more detailed scale, sediments can also

yield data, which can be used to infer the timing and rates of fault movement. Tectonic signatures at this scale can range from the character of individual sequences down to details of single beds. In a situation where the pattern of fault activity are poorly understood, recognisable responses in the sedimentary fill can provide the basis for tectonic interpretation (Frostick and Steel, 1993).

The Dead Sea rift, about 1000-km long, is the microplate boundary between Sinai (Levant) and the Arabian plate. Though it has many characteristics features of an extensional rift, this is a boundary of the transform type as it links the Dead Sea, where sea-floor spreading takes place, with the zone of continental collision in the Taurus-Zagros Mountains (Figure 1) (Garfunkel et al., 1981). Since the time of the Dead Sea formation in the Early Miocene, 105 km of left-lateral horizontal movement has occurred along its length (Freund et al., 1970). West of the basin, a major system of E-W strike slip faults has been mapped (Arkin et al., 1981). These faults cross and offset the major N-S trending normal faults, which define the western margin of the Dead Sea basin. The average slip rate in the last 4-5 m.y. is estimated to be 0.7-1.0 cm/y (Garfunkel et al., 1981).

Active faulting is easier to identify when young sediments are displayed, especially in semi-arid and arid climates. The majority of movements along the "Southern basin" Dead Sea rift are not sensational, but do nevertheless importance for long-term understanding of its origin and its activity.

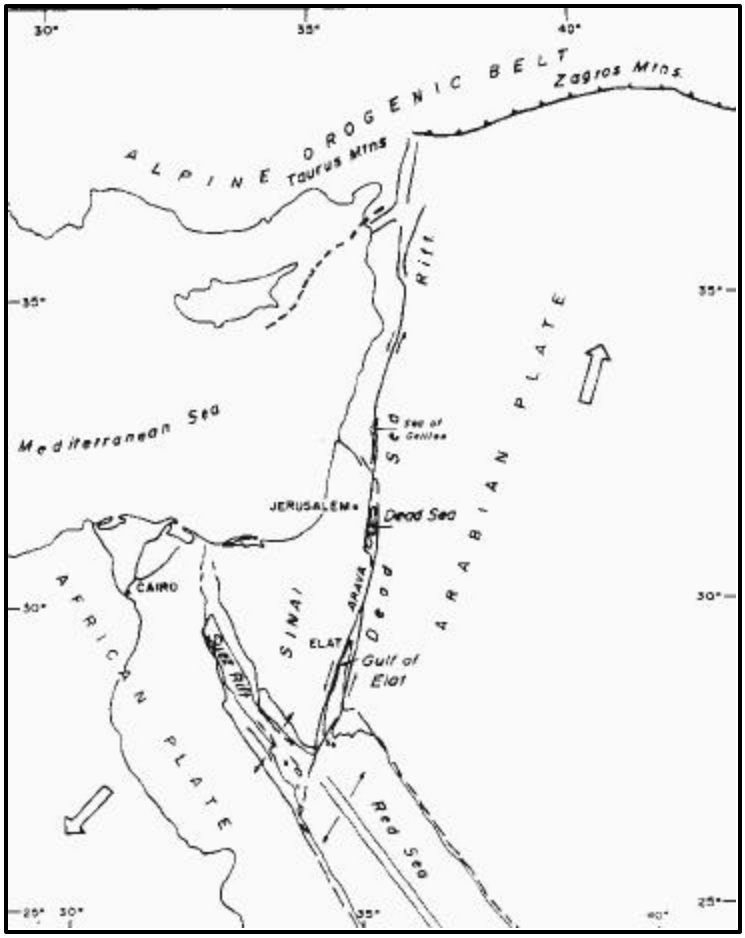

Figure 1: Plate tectonic setting of the Dead Sea rift (after Garfunkel et al., 1981).

Few studies used SAR interferometry to detect neotectonic activity in the Dead Sea rift, all of them focused on the reactivated fracture zones and corresponding displacement caused by the earthquake of November 1995 in the Golf of Aqaba (Baer et al., 1999; Bodechtel et al., 1997; Cornet et al., 1997). In this research the interferometry technique will be used to study the new displacements in different areas along the southern basin of the Dead Sea, but also to use high quality interferometric DEM to map the hydrographic network abnormalities which could be investigated on the tectonical point of view.

The hypothesis of this research is that combining optical data, physical features extracted from radar data and geophysical information can improve the understanding of neotectonical processes in the Dead Sea Rift. By analysing seven different seismic cross sections along the southern basin we studied the fault and fractures patterns in the depth. By extracting information using the DAIS sensor we mapped the lithological units. We will study the connection with the deep fracture patterns and the results extracted using the remote sensing tools. In this article we are presenting preliminary results of Amazijahu fault, one of the test site.

2 The Research Area

The "Southern basin" is part of the Dead Sea Rift, which is occupied by the Dead Sea (about 400 m below M.S.L.), and which is bordered by fault controlled escarpments breached by canyons. Many kilometres of mineralogy from the Pliocene-Quaternery age, mostly evaporites like halite, gypsum, anhydrite, aragonite, calcite and dolomite with interbedded clastics comprising clays, shales, sandston and quartz fill the segments of the rift. The southern basin of the Dead Sea extends from the Amatsyahu fault to north of the Lisan peninsula. Although much of the Jordan valley normal faults were probably not active in the post-lake Lisan time, the faults around the southern basin of the dead Sea could have moved at average rates of a few mm/y (Garfunkel et al., 1981).

The Amazijahu fault is a low-angle normal fault. The sedimentary infill above this fault is deformed by fractures and detached antithetic normal faults. The surface trace of the Amazijahu fault is curvilinear in the direction NW to NNW (Figure 2) and the escarpment retains a constant elevation along this trace (Brink and Ben-Avraham, 1989). Amazijahu is a very active fault and displacement can be expected three or even more time a year (like in the year 1987, 1988, 1989), with mean local magnitude of 3.2 (Israeli Geophysical Institution, 2000). The base of the escarpment is covered by Qaternary sediments of Samra and Lisan formations and younger Holocene deposits (Begin et al., 1980).

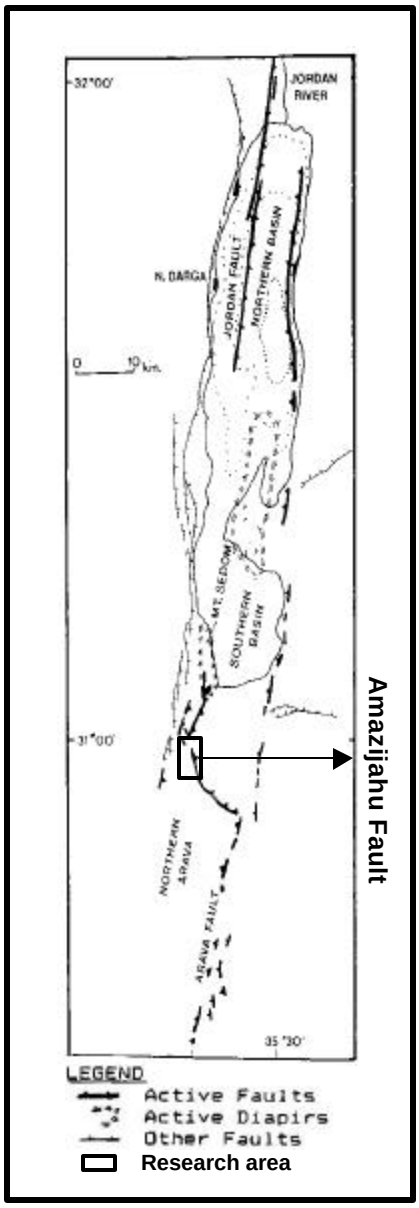

Figure 2: Active faulting in the southern Dead Sea basin (after Garfunkel et al., 1981).

3 Data set

3.1 Data from remote sensing instruments:

3.1.1 The Digital Airborne Imaging Spectrometer DAIS-7915. (DLR Germany) is a 79 channels high resolution optical spectrometer which collect information from the earth surface in the 0.4 µm to 12.3 µm wavelength with a spatial resolution of about 10 m. In August 1997 a research campaign using the DAIS-7915

was done over several places in Israel. This campaign was founded by the European Community and included five images covering a total area of 360 km^2 in the southern Dead Sea basin from an altitude of 10,000 m.

3.1.2 The European Remote Sensing Satellites ERS-1/2. Provides two-dimensional images with a spatial resolution of 12.5 m in range (across track) and in azimuth (along track). The radar obtains strip of high-resolution imagery of about 100 km width and operates in the C-band (5.3 GHz) with vertical polarisation. We acquired 32 ERS-1/2 tandem from the period 1992-1999, with different beams between 5 to 300 m, in the descending and the ascending paths.

3.2 Field data

The field campaign took place after the flight campaign and was initiated mainly for the calibration process. The samples were collected for the dominant lithological units. To spectrally characterize the collected field samples, laboratory spectrometer measurement with a LICOR (0.4-1.1mm) and LT-1200 (1.2-2.4mm) (Perkin Elmer Lambda 19 (0.5-2.4)) were performed.

3.3 Seismic reflection data

Numerous multichannel seismic profiles were collected and processed by oil companies over the last decade in the Dead Sea Basin. The profiles are usually of the highest quality available in the area in terms of both acquisition parameters and processing. The energy sources for the profiles were either Vibroseis system with 39-7 Hz sweep, 15-20 sweeps per vibrator point, or dynamite shots detonated simultaneously in 3-5 holes, 1-2 kg charge per hole. The profiles were recorded by 48 and 96 channel array, often in split profile configurations, with a typical recording time of 4-6 s. shot point and receiver station spacing varied between 36 m and 50 m. Profile line 7001 which is presented in this article is oriented E-W and crosses the Amazijahu fault where its intersects merges with the western longitudinal fault (Figure 2).

4 Methodology

For the general extraction of information from the different images, distinct processing steps are mandatory.

4.1 Processing of the DAIS-7915 data

4.1.1 Maximum noise fraction transform. Evaluation of the Amazijahu DAIS data revealed a high random and systematic noise content in the SWIR2 detector, with maximum SNR value of around 60:1. The MNF transform processing have been done based on raw data.

4.1.2 Radiance to reflectance conversion. The radiometric calibration was made using empirical line conversion approach, based on the laboratory spectrometer measurements. The linear regression was based on spectra of five locations, which had average low reflection (dark target) or high reflection (white target). Analysis of the resulting reflectance data revealed low remaining effect in the data.

4.1.3 Endmemember selection strategy. The Purity Pixel determination strategy was employed for the supervised classification. The PPI algorithm ranks every pixel in an image in terms of relative purity

through an iterative process of projection onto a random unit vectors in n-space. The potential endmembers spectrum was loaded into an n-dimensional scatterplot. Based on this strategy a number of 27 initial endmembers was defined.

4.1.4 Abundance mapping. Using the Linear Unmixing (UNM) processing we calculated the apparent fractional abundance of image-derived endmembers. This method determines the fractional abundance of each endmember, with the best fitting to the observed mixed spectrum at each pixel. It assumes that the reflectance of a given target is a combination of each target component reflectance (Ben-Dor et al., 1996).

4.1.5 Mineralogical mapping. We reduced the number of classes to 11 generalised classes based on similarity spectra and using clump post classification technique in GIS ArcInfo environment system. The final interpretation was made using ArcView environment.

4.2 Interferogram Processing

At this stage of the work only preliminary steps of the interferogram process have been made for twelve pairs. This is due to the high number of pairs, the correction of the orbit, atmosphere, temporal and baseline decorrelation effects and the quality assessment of each step in the interferogram process.

4.3 processing of the seismic profile

Standard exploration processing was applied to the seismic profile. In our analysis we used time migrated version of the profile. The interpretation have been published previously (Kashai and Crocker, 1987; Brink and Ben-Avraham, 1989).

Summary of the different processing stages are presented in Figure 3.

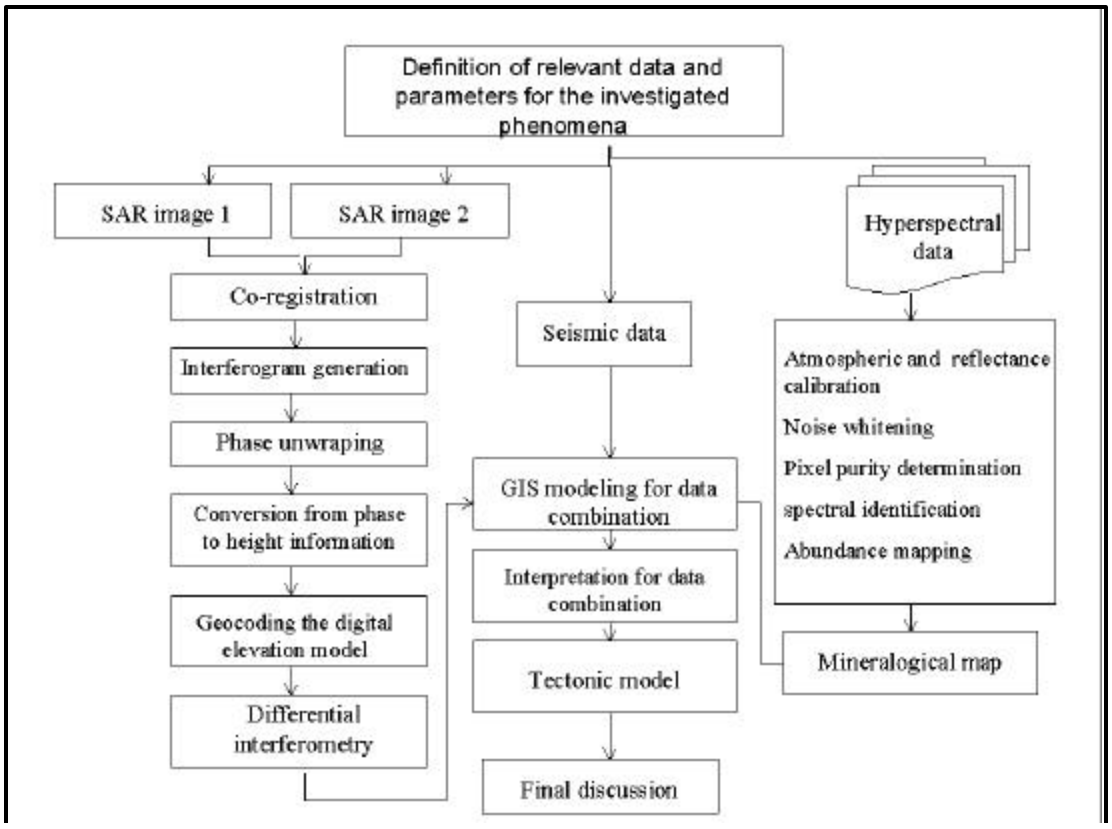

Figure 3: Summery of the different processing stages in the model

5 Results and Discussion

The results of the hyperspectral data are presented in Figure 4. The eleven classes were labelled according to their apparent bulk mineralogy as interpreted from mean DAIS class spectra. The lithological interpretation results supported by the Lisan lithology interpretation was made in the area by Begin et al. (1980). The lithology classification exposed in the southern part of the area, a rich carbonate zone with low clay content (mainly aragonite). There is a gradient from the south to the north in the clay content (marl) and rich gypsum zone was also exposed in the north.

North-western trending which implies the existence of other faults west to Amazijahu fault separates the southern lithological units. Examination of several air-photos exposed Amazijahu fault but did not manage to expose other faults western to it. However, in the SAR amplitude image produced in the preliminary steps of the interferogram process, a straight continuous northwest line appears west to Amazijahu fault.

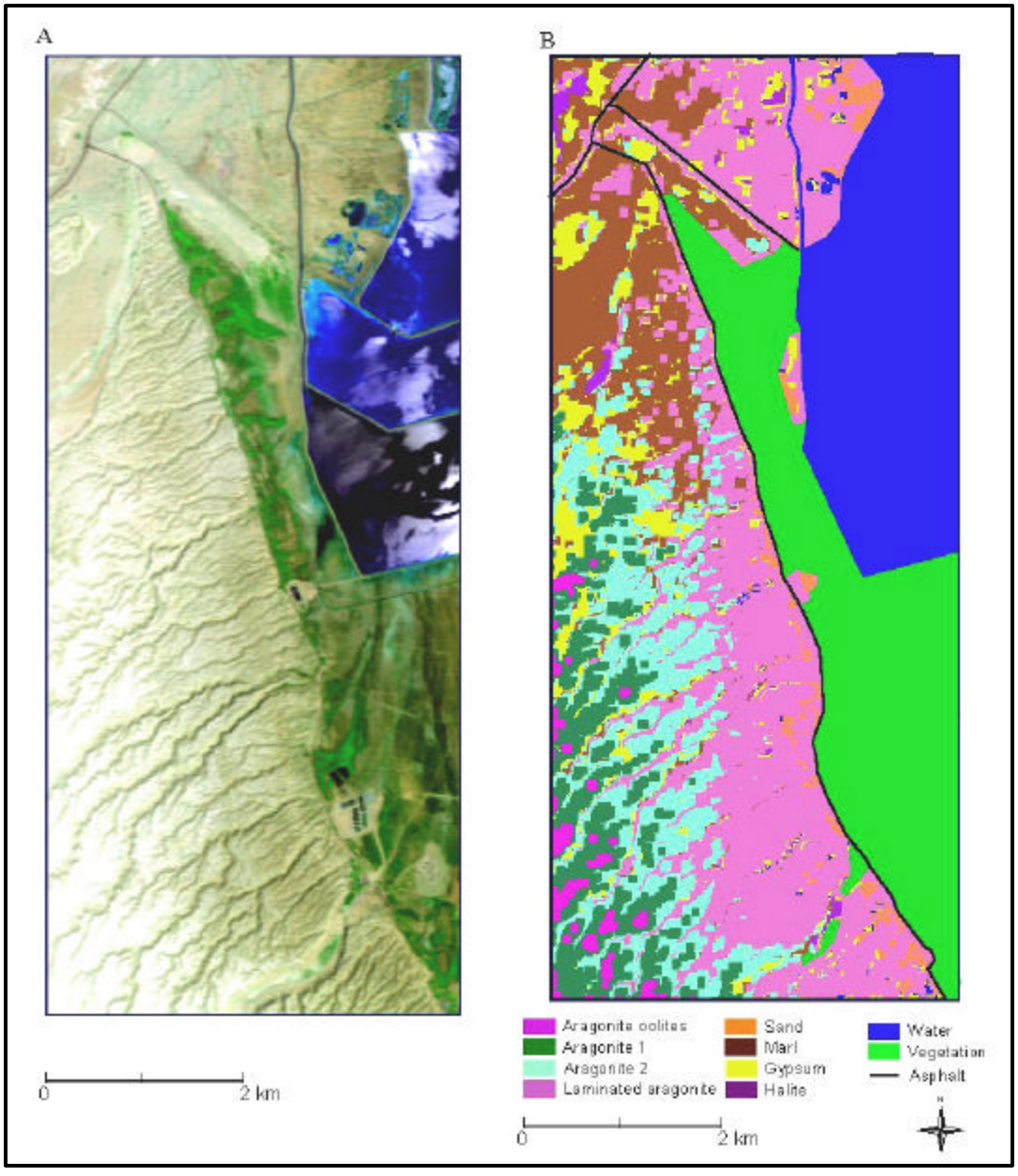

Figure 4: (A) False color composite (RGB) of channel 53, 25, 2 of DAIS-7915 data
(B) Classification result for Amazijahu fault.

The Amazijahu fault appears in the seismic reflection profile (Figure 5) as a low angle normal-fault, which may be traced from the surface down to a depth of 2.7 second two-way travel time. The basement underline the fault zone appears to be cut by normal fault which offset tilted block. We can notice that western to the Amazijahu fault appears another normal fault which connect to the Amazijahu in a depth of 2.3 second two-way travel time. Both of the faults progressive are steeping toward the west. The distance between the two faults near the surface is approximately 2 km.

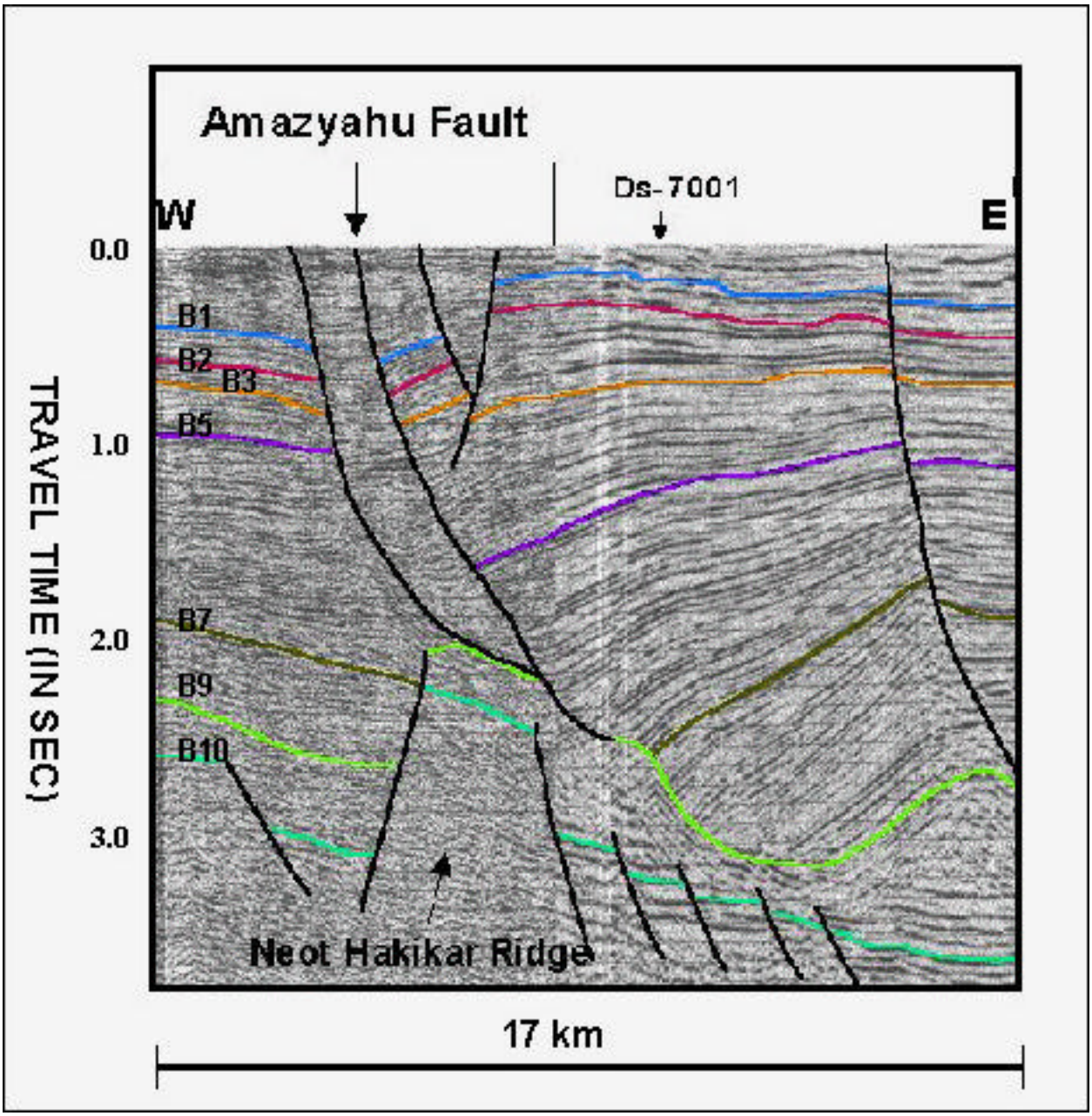

Figure 5: Migrated seismic line 7001 which cross the Amazijahu fault. B1-B10 sequence boundaries.

The different results were merged using GIS environment and the interpretation is presented in Figure 6. The interpretation show agreement between the fault exposed by the seismic and the SAR data with the spatial distribution of the lithological units revealed by the hyperspectral data. However, the DAIS classification

exposed several units separated by northwest trending while the seismic and the SAR data exposed only one fault western to Amazijahu. To verify the results and to find what is the connection between the lithological unit and the neotectonic processes, further investigation and field validation work have to be done. In this respect, hydrographic and shallow seismic profile investigations have to be done to support the results.

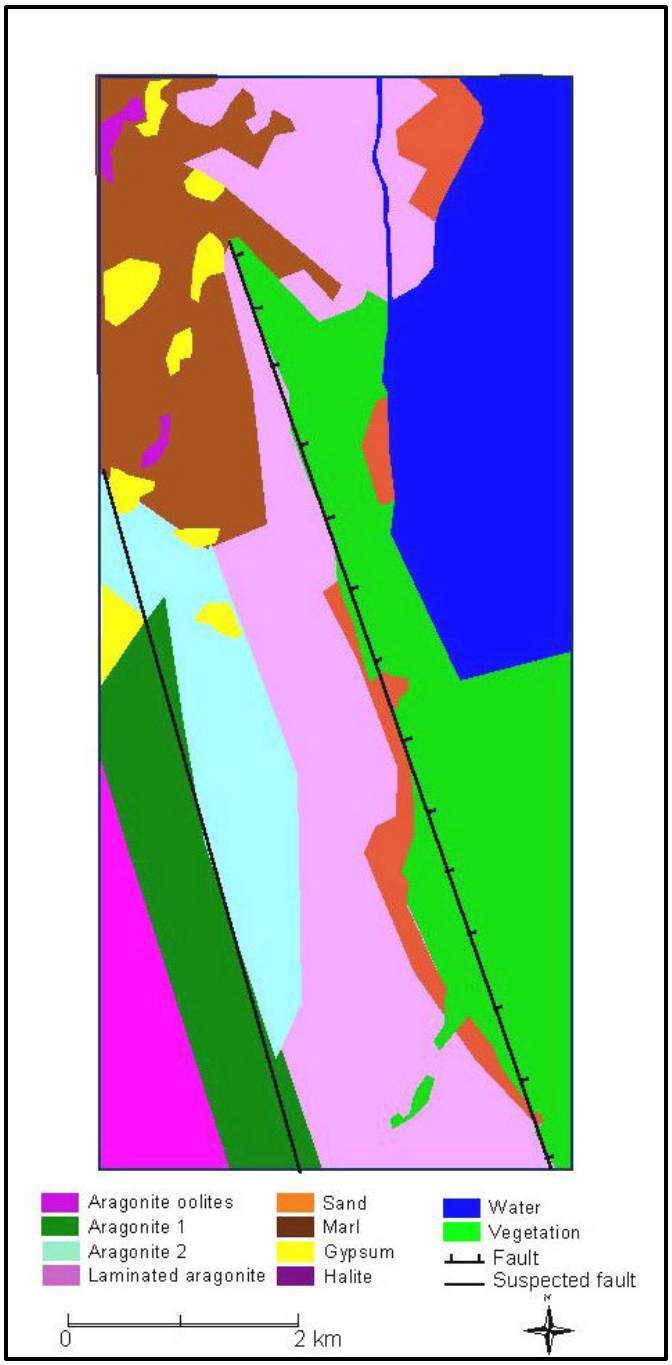

Figure 6: Interpretation of the combined results.

6 Conclusions

This research proposed a model detecting neotectonic process in the Dead Sea rift, Israel. Although the results are preliminary, agreement was found between seismic activity in the rift and the lithological units distribution.

The research also proves again the possibility to produce high quality lithological mapping using the DAIS-7915. Further investigation and field validation have to be done.

7 Acknowledgements

The authors would like to thank the DLR and GFZ (Germany) for acquiring and supplying the DAIS-images, NUFFIC (Holland) and Renaissance (Belgium) for the financial support. The authors also wish to thank Prof. Ben-Avraham, Z. and Lazar, M. from the geophysical department in Tel-Aviv university for the interest and the support in this research. We extend our thanks to Sirjacobs, D. who provided timely and efficient support in the manuscript proof.

8 References

Arkin, Y., Gilat, A. and Agnon, A., (1981), Mediterranean-Dead Sea project: Geotechnical survey of area proposed for an underground power station., Geol. Surv. Isr. Rep. MM/3/81, 15 p.

Baer, G., Sandwell, D., Williams, S. and Bock, Y., (1999), "Coseismic deformation associated with the November 1995, Nw = 7.1 Nuweiba earthquake, Gulf of Eilat (Aqaba), detected by synthetic aperture radar interferometry", J. Geophys. Res., 104, B-11, 25221-25232.

Begin, Z. B., Nathan, Y. and Erlich, A., (1980), "Startigraphy and facies distribution in the Lisan formtion – New evidence from the area south of the dead Sea, Israel", Isr. J. Erth. Sci., 29: 182-189.

Ben-Dor, E., Kruse, F. A., Dietz, J.B., Braun, A. W. and Banin, A. (1996). "Spatial distortion and quantitative geological mapping of Makhtesh Ramon, Negev, Israe, by using the GER 63 channel scanner data". Canadian J. of Remote Sensing. Vol. 22, 3, Pp. 258-268.

Bodechtel, J., Frei, M., Tretter, W., Wever, T., Kauffman, H., Xia, Y. and Beyth, M., (1997), "Multisensoral approach for studying the geology and tectonics of the Dead Sea rift, Israel", Proceeding of IGARSS'97, Barcelona, CD.

Brink, U. and Ben-Avraham, Z., (1989), "The anatomy of a pull-apart basin: seismic reflection observations of the Dead Sea Basin", Tectonics, 8: 333-350.

Cornet, Y., Doulliez, J. Y., Moxhet, D., Closson, D., Kourgli, A. and Ozer, A., (1997), "Use of ERS tandem data to produce digital elevation models by interferometry and study land movements by differential interferometry in Calabria and Jordan", ERS Symp. Interferometry, Florence, CD.

Frostick, L. E. and Steel, R. J., (1993), Tectonic control and signatures in sedimentary succession, Blackwell scientific publication, Oxford, 270 pp.

Freund, R., Garfunkel, Z., Zak, I., Goldberg, M., derin, B. and Weissbord, T., (1970), "The shear along the Dead Sea rift", Philos. Trans. R. Soc. London, Ser. A., 267: 107-130.

Garfunkel, Z., Zak, I. and Freud, R., (1981), "Active faulting in the Dead Sea rift", Tectonophysics, vol. 80, pp. 1-26.

Kashai, E.L. and Crocker P. F., (1987), "Structural geometry and evolution of the Dead Sea-Jordan rift system as deduced from new subsurface data", Tectonophysics, 141, 33-60.